Study of the Fiber Bragg's Grating Sensor Sensibility Subjected to Harsh Environmental Conditions

LUDOVIC GAVERINA, ANASTASIA LIAPI,
JESUS EIRAS FERNANDEZ, EMMANUEL MARIN,
JEREMY RIPORTO, JEOFFRAY VIDALOT,
SYLVAIN GIRARD and JEAN-MICHEL ROCHE

ABSTRACT

This study investigates the performance of Fiber Bragg Grating sensors bonded with an cyanoacrylate adhesive to different substrate materials (titanium, aluminum, and carbon-fiber-reinforced polymers) for Structural Health Monitoring applications in the aeronautical industry. The results show that thermal aging alters the adhesive layer, ultimately modifying the FBG sensor's sensing ability. A finite element model is used to study the most influential factors on the bonding agent and FBG sensor durability.

INTRODUCTION

Aircraft health assessment relies on regular inspections, which can be costly and lead to unnecessary shutdowns if no actual damage is found. Condition-based maintenance (CBM) using Structural Health Monitoring (SHM) systems is a more cost-efficient solution. Fiber Bragg Grating (FBG) sensors [1,2] are appealing for SHM applications because they are lightweight and can provide various measurements. However, harsh environmental conditions such as exposure to high and low temperatures, UV radiation, and mechanical vibration can degrade the sensor bonding, which can lead to inaccurate SHM data. A high-integrity bond between the FBG sensor and the structure is essential for long-term operation.

This study investigates the performance of FBG sensors bonded with an cyanoacrylate adhesive (M-Bond 200) to different substrate materials (titanium, aluminum, and carbon-fiber-reinforced polymers). Testing coupons were prepared and subjected to thermal cycling from 50°C up to 180°C to accelerate aging. The FBG response was monitored during the aging testing. Results showed that thermal aging

Gavérina L. DMAS, ONERA, Paris-Saclay University, F-92322 Châtillon, France. ONERA, 29 Av. de la Division Leclerc, 92320 Châtillon, France

altered the integrity of the adhesive layer and modified the sensing ability of the FBG sensor. Physical properties of the adhesive, such as thickness, elastic properties, and density, were weakened during thermal treatment. A finite element model (FEM) was implemented to model the experimental observations. A parametric sensitivity study was conducted to identify the most influential factors on bonding agent and FBG sensor durability.

Overall, this study highlights the importance of having a high-integrity bond between FBG sensors and the structure to acquire accurate SHM data. Additionally, the study identifies factors that impact bonding agent and FBG sensor durability and provides insights on how to improve their performance under harsh environmental conditions. By addressing these issues, CBM using SHM systems can become a more cost-efficient solution for aircraft health assessment, reducing the need for costly periodic inspections and increasing aircraft availability.

METHODOLOGY

In this study, the spectrum reflected by the Bragg grating is recorded over time by a spectrometer. In the case where the fiber is subjected to thermomechanical stress, the grating pitch is modified, resulting in a variation of the Bragg wavelength. The three physical quantities that influence the Bragg grating are the temperature T, the mechanical strain ε, and the pressure P [3]. In our study, the pressure is not taken into account as it has little effect on the grating.

$$\frac{\Delta\lambda_B}{\lambda_B} = S_T \Delta \mathrm{T} + S_\varepsilon \varepsilon + S_P \Delta \mathrm{P} \quad (1)$$

We propose to represent these spectra recorded over time in the form of a spectrogram. Throughout the article, we will use the term "GAVgram" (**G**rating **A**nalysis **V**ariation) to refer to this presentation of the spectra. The columns of the GAVgram represent the variations of the spectrum during the test, and the rows represent the amplitude of the spectrum reflected by the Bragg grating, as illustrated below.

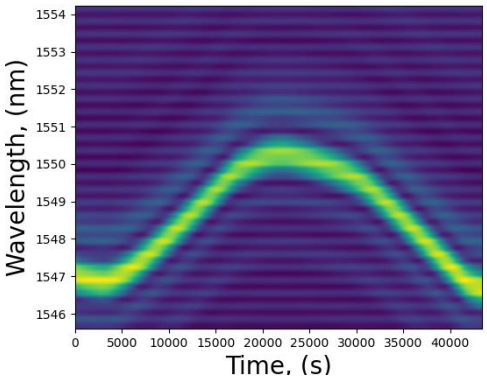

Figure 1. GAVgramm representing the variation of the Bragg wavelength of an FBG subjected to temperature variations.

THERMOMECHANICAL ANALYSIS

The RTCA DO-160 is a standard used for testing the temperature variations of internal and external devices on aircraft, ranging from the lowest to highest expected operating temperatures. In this study, the SHM systems were subjected to a thermal cycling test with a temperature variation rate of 3 degrees Celsius per minute. The temperature range varied between 50°C and 160°C [4] and was maintained for 10 minutes (Figure 2). This thermal cycling is crucial to determine the performance of the SHM systems in harsh environments, as aircraft structures are commonly exposed to high and low temperatures. The temperature variations during the test were represented by the columns in a Gavgram plot, while the lines in the plot represented the amplitude of the spectrum reflected by the Bragg grating. Overall, the thermal cycling test was used to assess the durability and reliability of the SHM systems under harsh temperature conditions, with the aim of ensuring safe and efficient operation of aircraft structures.

a)

b)

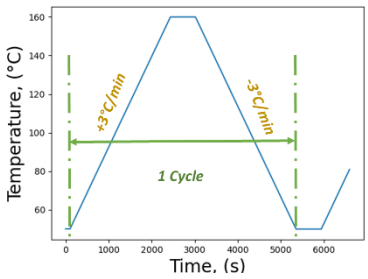

Figure 2. a) Photo of the climatic chamber used for conducting thermal cycling, and b) a graphical representation of the thermal cycle for conducting aging.

A two dimensional finite element thermal model has been developed using COMSOL Multiphysics® software to understand the thermo-mechanical phenomena. Figure 3 displays the simulated geometry.

For this work, the following parameters are used:

- aluminium properties : Young's modulus of 69 GPa, thermal expansion of $23.4*10^{-6}$ K^{-1}
- Araldite properties : Young's modulus of 1.85 GPa, thermal expansion of $1.27*10^{-7}$ K^{-1}
- Optical fiber properties : 200µm diameter, Young's modulus of 49 GPa, thermal expansion of $0.55*10^{-6}$ K^{-1}
- adaptive structured mesh (grid of 1,080 elements).

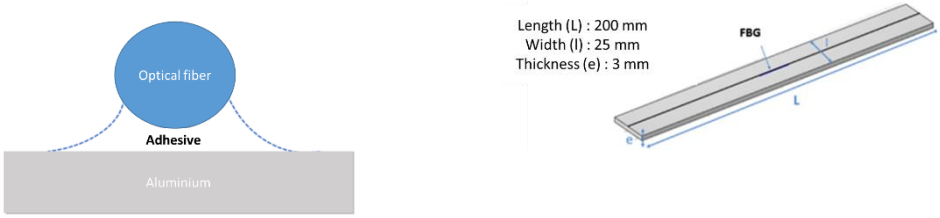

Figure 3. Geometry of the numerical simulation: FBG, adhesive and Aluminium

On the figure below, the principal stresses in x (left) and y (right) directions are represented. In Figure 4a), the thermal loading induces a tensile stress of around 2.5×10^8 N/mm^2 in the fiber direction. In Figure 4b), a tensile stress of around 6×10^7 N/mm^2 is observed in the y-direction perpendicular to the fiber axis at the interface between the adhesive joint and the fiber. In contrast, the aluminum experiences a compressive stress of around 2×10^7 N/mm^2. The existence of two different states of stresses (tensile and compressive) may cause shear stresses to appear at the interface between the fiber/adhesive/aluminum, which can lead to structural damage.

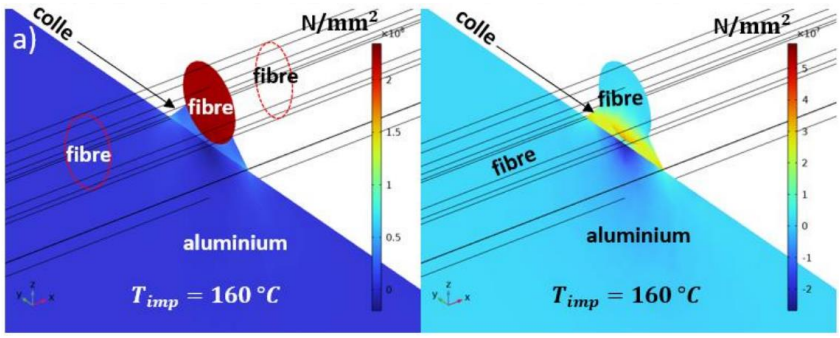

Figure 4. Thermal loading on a fiber bonded to an aluminum specimen: a) stress on the fiber section along x, b) stress on the adhesive-fiber interface along y."

ANALYSIS ESTIMATION OF THE BRAGG'S WAVELENGTH

In the scientific literature, numerous methods exist for estimating the Bragg length, such as calculating the centroid, minimizing the Bragg's wavelength using a Gaussian or cardinal sine function, etc. [5]. We propose a new method by approximating the Bragg length with a Gaussian function equation (1) [6]. This method is explained below.

The equation (1) can be transformed into a logarithmic expression, which can be further developed into a second-order polynomial equation (2) containing three coefficients that depend on the wavelength.

$$S(\lambda) = A * \exp\left(-\frac{(\lambda-\lambda_B)^2}{2*\sigma^2}\right) \quad (1)$$

With λ_B the Bragg's wavelength and A the amplitude

$$log\big(S(\lambda)\big) = log(A) - \frac{\lambda}{2\sigma^2} + \frac{\lambda\lambda_B}{\sigma^2} + -\frac{{\lambda_B}^2}{2\sigma^2} \quad (2)$$

By identifying the parameters:

$$y = a\lambda^2 + b\lambda + c$$
$$\begin{cases} a = -\frac{1}{2\sigma^2} \\ b = \frac{\lambda_B}{\sigma^2} \\ c = log(A) - \frac{{\lambda_B}^2}{2\sigma^2} \end{cases} \quad (3)$$

The Bragg wavelength is given by $\lambda_B = \frac{-b}{2a}$

DISBONDING DETECTION

A uniaxial monotonic tensile test was conducted at room temperature (25 °C). This test validates that after debonding, the FBG no longer follows the deformation of the aluminum specimen. The tensile test is performed using an Instron tensile testing machine (Model E3000) capable of applying traction/compression tests up to $\pm 3000N$ with maximum displacements of $\pm 30\ mm$.

The aluminum specimen is rectangular with the following dimensions: length (L) of 200 mm, width (l) of 25 mm, and thickness (e) of 3 mm. To verify if the FBG accurately tracks the deformation of the specimen, a strain gauge is positioned near to the FBG.

In the figure below, the Bragg's wavelength of the FBG is plotted when a maximum stress of 3 kN is applied. This measurement is compared to the estimation

from a strain gauge. It can be observed that the Bragg wavelength follows the deformation of the aluminum specimen which confirms that the FBG is properly bonded to the specimen and does not exhibit any debonding.

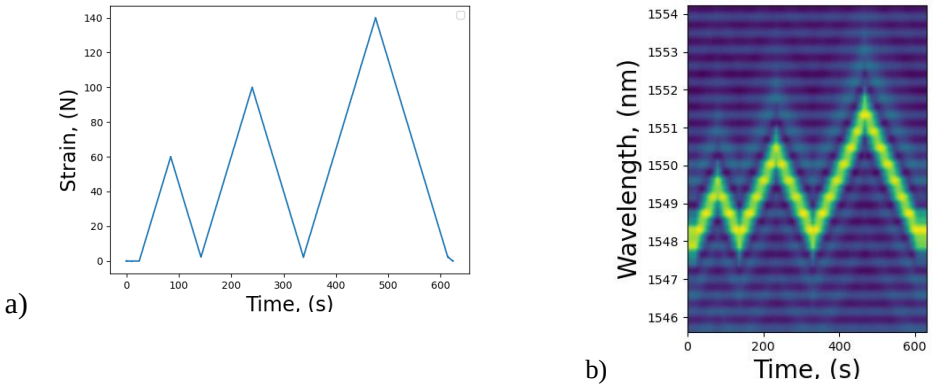

Figure 5. Mechanical testing: a) loading and unloading, b) spectral response of the FBG.

Following these initial tensile tests, the specimen underwent aging cycles according to the RTCA DO-160 standard (see Figure 2). The duration of these cycles was 12 hours. Real-time acquisition was performed using an IBSEN spectrometer (I-MON512).

Below is illustrated the result of the acquisitions during the thermal cycling. It is possible to observe in the GAVgram of the first cycle a shift in the Bragg wavelength. This singularity illustrates the debonding of the FBG from the specimen as the grating is no longer constrained by the adhesive. During the curing of the adhesive, the grating pitch decreases, resulting in a decrease in the Bragg wavelength as well. However, it can be noted that after debonding, the wavelength follows the temperature. The Bragg grating now measures only one physical quantity: the temperature.

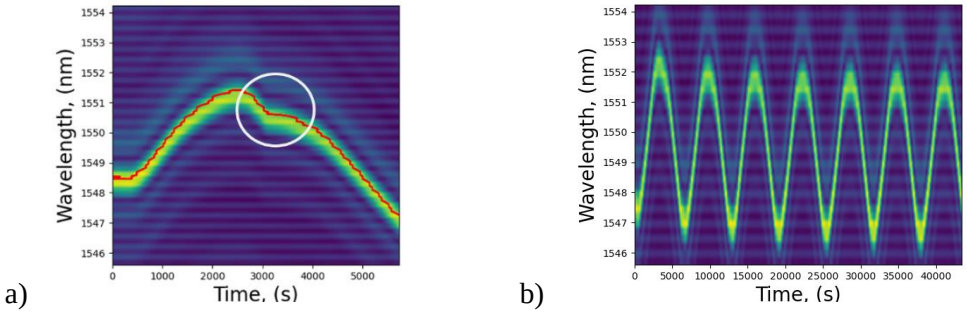

Figure 6. Spectral response of the FBG after thermal aging: a) debonding, b) post-debonding response of the FBG

To verify that the Bragg grating is detached from the specimen, a tensile test was performed on the aged specimen. The test was conducted with 3 cycles of a 3 kN stress, and the reflected spectrum by the Bragg grating was acquired in real-time. Based on the results illustrated in Figure 7, it can be observed that the shift in the Bragg wavelength does not emerge from the measurement noise. The grating does not follow the deformation of the specimen anymore, which confirms that it is indeed detached from the specimen.

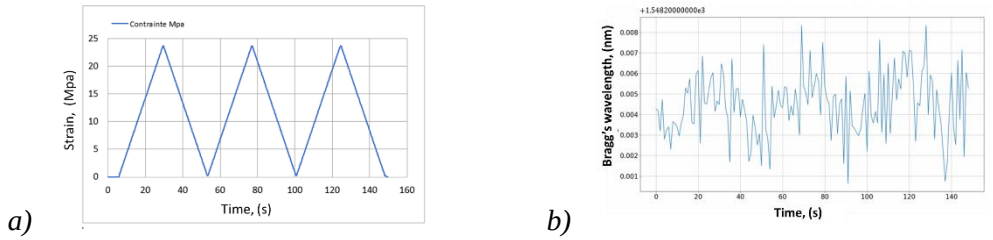

a) *b)*

Figure 7. Mechanical test after FBG debonding: a) loading and unloading, b) spectral response of the FBG.

CONCLUSION

This study investigated the performance of Fiber Bragg Grating (FBG) sensors bonded with an cyanoacrylate adhesive to aluminum substrates for Structural Health Monitoring (SHM) applications in the aeronautical industry. The results demonstrated that thermal aging adversely affects the adhesive layer and modifies the sensing ability of FBG sensors. In response, an innovative methodology for detecting FBG failures has been developed. The GAVgrams, which represent spectral variations over time, enable direct detection of these anomalies. By analyzing the GAVgrams, significant deviations in the Bragg wavelength can indeed be identified, indicating an FBG failure. This approach provides a visual and intuitive method for real-time monitoring of sensor integrity, effectively detecting issues such as debonding or adhesive degradation. The use of GAVgrams facilitates preventive maintenance by enabling early anomaly detection, thereby enhancing the safety and reliability of structural monitoring systems that employ FBG sensors. This methodology opens up new possibilities for efficient and effective FBG-based structural health monitoring.

REFERENCES

1. Goossens, S., De Pauw, B., Geernaert, T., Salmanpour, M. S., Sharif Khodaei, Z., Karachalios, E., Saenz-Castillo, D., Thienpont, H., & Berghman, F. (2019). "Aerospace-grade surface mounted optical fibre strain sensor for structural health monitoring on composite structures evaluated against in-flight conditions." Smart Materials and Structures, 28(6), 065008.
2. Speckmann, H., & Henrich, R. (2004, August). "Structural health monitoring (SHM) – overview on technologies under development." In Proceedings of the 16th World Conference on NDT (Vol. 1)
3. Fernando, G. F., Webb, D. J., & Ferdinand, P. (2002). "Optical-fiber sensors." Mrs Bulletin, 27(5), 359-364.
4. Gavérina, L., Roche, J. M., Beauchêne, P., & Passilly, F. (2021). "Study of the Effects of Thermal Stress on Piezoelectric Sensors for the Structural Health Monitoring." STRUCTURAL HEALTH MONITORING 2021.
5. Demirel, M. (2009). Contribution à l'optimisation des mesures de température et de déformations par capteur à fibre optique à réseau de Bragg: application au procédé de fabrication des composites par infusion de résine (Doctoral dissertation, Saint-Etienne, EMSE).
6. Gaverina, L., Batsale, J. C., Sommier, A., & Pradere, C. (2017). "Pulsed flying spot with the logarithmic parabolas method for the estimation of in-plane thermal diffusivity fields on heterogeneous and anisotropic materials." Journal of Applied Physics, 121(11), 115105.